

LETTER TO THE EDITOR

## *Planck* confirmation of the disk and halo rotation of M 31

F. De Paolis<sup>1,2</sup>, V. G. Gurzadyan<sup>3</sup>, A. A. Nucita<sup>1,2</sup>, G. Ingrosso<sup>1,2</sup>, A. L. Kashin<sup>3</sup>, H. G. Khachatryan<sup>3</sup>, S. Mirzoyan<sup>3</sup>,  
E. Poghosian<sup>3</sup>, Ph. Jetzer<sup>4</sup>, A. Qadir<sup>5</sup>, and D. Vetrugno<sup>6</sup>

<sup>1</sup> Dipartimento di Matematica e Fisica “E. De Giorgi”, Università del Salento, via per Arnesano, 73100 Lecce, Italy  
e-mail: francesco.depaolis@le.infn.it

<sup>2</sup> INFN, Sez. di Lecce, via per Arnesano, 73100 Lecce, Italy

<sup>3</sup> Yerevan Physics Institute and Yerevan State University, 375049 Yerevan, Armenia

<sup>4</sup> Physik-Institut, Universität Zürich, Winterthurerstrasse 190, 8057 Zürich, Switzerland

<sup>5</sup> Centre for Advanced Mathematics and Physics, National University of Sciences and Technology, 46000 Rawalpindi, Pakistan

<sup>6</sup> Department of Physics, University of Trento and TIFPA/INFN, 38123 Povo, Italy

Received 20 March 2014 / Accepted 15 April 2014

### ABSTRACT

*Planck* data acquired during the first 15.4 months of observations toward both the disk and halo of the M 31 galaxy were analyzed. We confirm the temperature asymmetry that was previously detected by using the seven-year WMAP data in the direction of the rotation of M 31, which indicates that this is a Doppler-induced effect. The asymmetry extends to about  $10^\circ$  ( $\approx 130$  kpc) from the center of M 31. We also investigated the recent problem raised in Rubin and Loeb (2014, JCAP, 01, 051) about the kinetic Sunyaev-Zel’dovich effect from the diffuse hot gas in the Local Group, which is predicted to generate a hot spot of a few degrees in size in the cosmic microwave background maps in the direction of M 31, where the free electron optical depth is highest. We also considered whether the same effect in the opposite direction with respect to the M 31 galaxy induces a minimum in temperature in the *Planck* maps of the sky. We find that the *Planck* data at 100 GHz show an even stronger effect than that expected.

**Key words.** galaxies: general – galaxies: individual: M 31 – galaxies: halos

### 1. Introduction

Galactic disk rotation can be accurately investigated in the optical, infrared (IR), and radio bands and allows one to infer important information, among others, about the dynamical mass content of galaxies (see e.g. Binney & Merrifield 1998). But our knowledge of the main constituents of galactic halos is still incomplete. Ascertaining the degree to which galactic halos rotate with respect to the disks is a particularly difficult task to accomplish, even for the closest galaxy to the Milky Way: M 31 (Courteau et al. 2011). A novel approach in studying the rotation of the disk and halo of nearby galaxies (particularly the M 31 galaxy) has been discussed in De Paolis et al. (2011). By using the seven-year WMAP data, a possible temperature asymmetry was found both in the M 31 disk and in the halo in the direction of the rotation of M 31, which indicates a Doppler-induced effect. By adopting the geometry described in Fig. 1 in De Paolis et al. (2011) and extending the analysis to about  $20^\circ$  ( $\approx 260$  kpc) around the center of M 31, we found a temperature difference of about  $130 \mu\text{K}$  in the two opposite regions of the M 31 disk that was about equal in the *W*, *V*, and *Q* WMAP bands. A similar effect was also visible toward the halo of M 31 up to about 120 kpc from the center of M 31 with a peak value of about  $40 \mu\text{K}$ . The robustness of this result was tested by considering 500 randomly distributed control fields and also by simulating 500 sky map realizations from the best-fit power spectrum constrained with BAO and  $H_0$  (see De Paolis et al. 2011, for details). The probability that the detected temperature asymmetry toward the disk of M 31 is due to a random fluctuation of the cosmic microwave background (CMB) signal is below about 2%, while for the halo of M 31 it is less than about 30%. Although the confidence level of the signal was low in the WMAP data, if one

considers only the statistics, nevertheless, we believed that the geometrical structure of the temperature asymmetry indicated a definite effect modulated by the rotation of the disk and halo of M 31 and suggested that it might be possible to definitely prove or disprove our conclusions with *Planck* data. The *Planck* satellite is about ten times more sensitive than the WMAP satellite and has an angular resolution about three times better: the *Planck* full width at half maximum (FWHM) resolution ranges from  $33.3'$  to  $4.3'$ , from 30 GHz to 857 GHz, and its final sensitivity is in the range of  $2$ – $4.7 \mu\text{K}/\text{K}$  in terms of  $\delta T/T$  for the Low-Frequency Instrument (LFI), which has a range of 30–70 GHz, and of  $2$ – $14 \mu\text{K}/\text{K}$  for the High-Frequency Instrument (HFI) below 353 GHz (see e.g. Burigana et al. 2013, for a recent review on *Planck* results). Our aim here is therefore to analyze the *Planck* data acquired during the first 15.4 months of observations toward both the disk and halo of the M 31 galaxy in detail. In addition, we also take the opportunity of investigating in some detail the recent question raised in Rubin & Loeb (2014) about the kinetic Sunyaev-Zel’dovich effect from the diffuse hot gas in the Local Group, which is detected as a hot spot of a few degrees in size in the direction of M 31 (where the free electron optical depth is highest). We also investigated whether the same effect induces a minimum in temperature in the *Planck* maps of the sky in the opposite direction with respect to the M 31 galaxy.

### 2. *Planck* analysis

Two instruments are on board the *Planck* satellite: the LFI (Bersanelli et al. 2010) covers the 30, 44, and 70 GHz bands by using amplifiers cooled to 20 K. The HFI (Lamarre et al. 2010) covers the 100, 143, 217, 353, 545, and 857 GHz bands

**Table 1.** Temperature excess in the regions of M 31.

$R$ , deg, kpc	Region	$N$ , pix	$T_m \pm SE$	$T_m \pm \sigma$ for 360 control fields
1.5, 19.5	M1	4213	$115.4 \pm 2.0$	$44.0 \pm 5.0$
1.5, 19.5	M2	4182	$48.2 \pm 2.0$	$50.0 \pm 6.0$
4.0, 51.9	M1	29076	$70.1 \pm 0.9$	$41.0 \pm 7.0$
4.0, 51.9	M2	28983	$32.0 \pm 0.9$	$66.0 \pm 10.0$
4.0, 51.9	N1+S1	27957	$70.0 \pm 1.0$	$41.0 \pm 7.0$
4.0, 51.9	N2+S2	27874	$32.2 \pm 1.0$	$66.0 \pm 9.0$
10.0, 131.2	N1+S1	158752	$65.0 \pm 0.2$	$43.0 \pm 8.0$
10.0, 131.2	N2+S2	158720	$52.2 \pm 0.2$	$73.0 \pm 10.0$
4.0, 51.9	M 31	61306	$50.1 \pm 0.3$	$44.6 \pm 1.6$
4.0, 51.9	anti M 31	61306	$-6.2 \pm 0.3$	$24.8 \pm 1.0$

**Notes.** The radius of the annulus considered is given in degrees and in kpc in the first column; the value of 744 kpc (Vilardell et al. 2010) is adopted for the distance to M 31. The second column indicates the region considered. In the third column the numbers of pixels in each region are given. The fourth column shows the CMB mean temperature of each region (in  $\mu\text{K}$ ) in the 100 GHz *Planck* map with the corresponding standard error (SE), while the last column gives the average temperature excess in the 360 control fields with the standard deviation (see text for details).

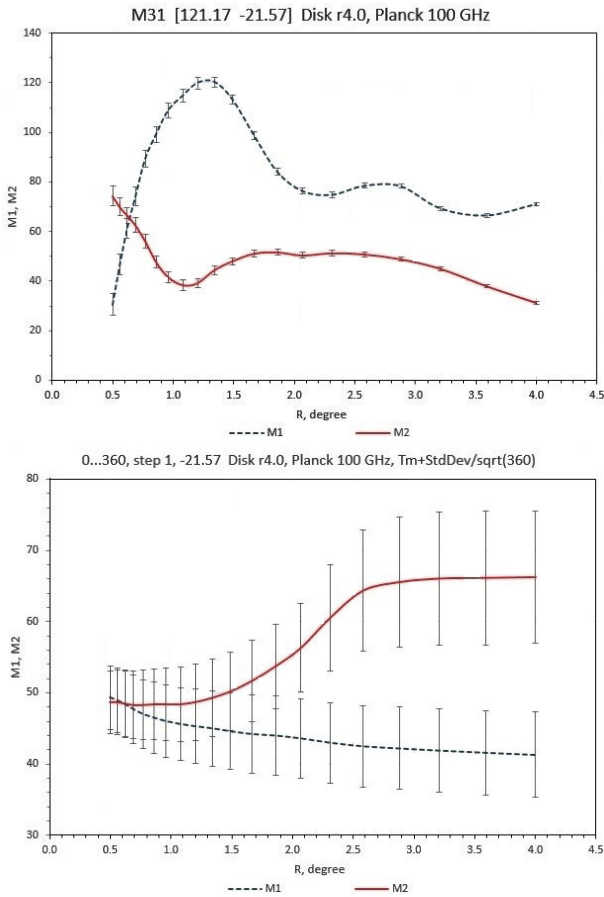


**Fig. 1.** *Upper panel:* excess temperature profiles (in  $\mu\text{K}$ ) for regions M1 and M2 of the disk of M 31. *Bottom panel:* temperature profiles (in  $\mu\text{K}$ ) for 360 regions equally spaced at one degree distance to each other in longitude and at the same latitude as M 31.

with bolometers cooled to 0.1 K. The sensitivity, angular resolution (from 3' to 5'), and frequency coverage of *Planck* make it a powerful instrument for cosmology as well as galactic and extragalactic astrophysics (Planck Collaboration 2012). To reveal the different contributions by the disk and halo of M 31, the region of the sky around the M 31 galaxy has been divided into several concentric circular areas, as shown in Fig. 1 in De Paolis et al. (2011), to which we refer for further details. Here we

only mention that the region M1 is the southeast half-disk of M 31, while region M2 corresponds to the northwest half-disk. Because of the disk of M 31 is rotating in clock-wise direction, we expect that the M1 region is hotter than that of M2. The mean temperature excess  $T_m$  in  $\mu\text{K}$  in each region was obtained in each *Planck* band and is shown in Table 1 with the corresponding standard error (SE)<sup>1</sup>, along with the number of pixels in each area.

## 2.1. Results for the disk of M 31

Region M1 of the disk of M 31, as can be seen from the first four lines of Table 1 and Fig. 1, is always hotter than the region M2. For example, at 1.5° region M1 is 67  $\mu\text{K}$  hotter than region M2 and even at 4° the region M1 is 38  $\mu\text{K}$  hotter than region M2. The upper panel of Fig. 1 clearly shows the temperature asymmetry profile in the two regions of the disk of M 31. These profiles agree with the results obtained previously by using the WMAP data (De Paolis et al. 2011)<sup>2</sup>. Moreover, the shape of the two profiles is clearly mirrored, as expected if the effect is due to a Doppler modulation induced by the rotation of the M 31 disk. The hotter (M1) region corresponds to the side of the M 31 disk that rotates toward Earth. This mirrored shape of the two regions of the disk of M 31 is also visible in the M 31 thick HI disk obtained at 21 cm (Chemin et al. 2009; Corbelli et al. 2010). To test whether the temperature asymmetry we see toward the disk of M 31 is real or can be explained as a random fluctuation of the CMB signal (which is very patchy) we adopted a different strategy than that in De Paolis et al. (2011). We considered 360 control field regions with the same shape as the regions M1 and M2 and at the same latitude as M 31, but at 1° longitude from

<sup>1</sup> The standard error given in the fourth column is calculated as the standard deviation of the excess temperature distribution divided by the square root of the pixel number in each region. To enable the comparison with the previous WMAP data analysis (De Paolis et al. 2011), here we used *Planck* 100 GHz data and have verified that within the errors, the sigma values calculated in that way are consistent with those evaluated by using the covariance matrix obtained by a best-fitting procedure with a Gaussian to the same distribution. In the last column we give the average excess temperature for 360 control fields with the usual standard deviation.

<sup>2</sup> The absence of foreground-reduced *Planck* maps, which were available for WMAP maps, makes the comparison between real and simulated data ambiguous. The strategy adopted here of using 360 control fields in the *Planck* maps gives more reliable results.

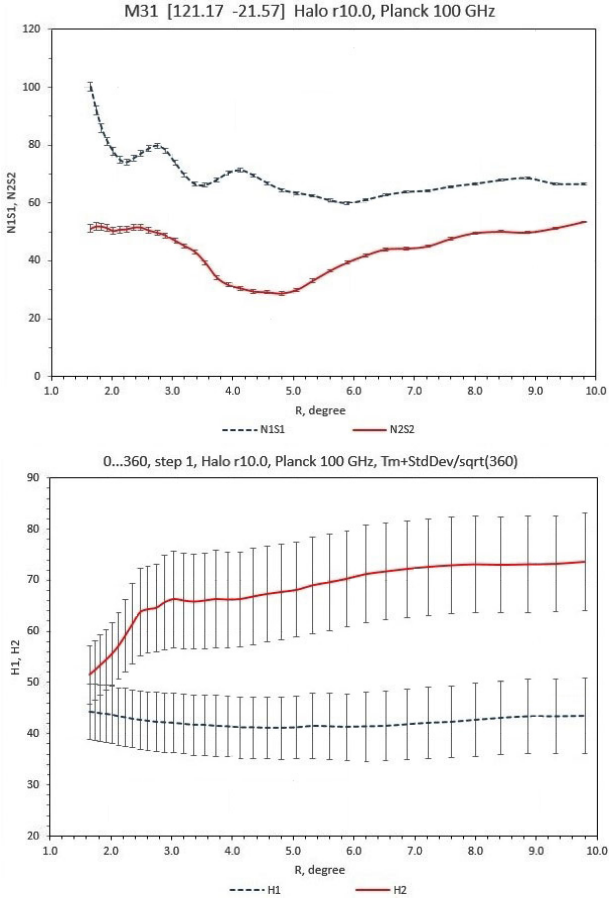


**Fig. 2.** Same as for Fig. 1, but for the halo of M 31 (*upper panel*) and for 360 regions at one degree of longitudinal distance to each other ( $H = N + S$ , *bottom panel*).

each other. For each region we determined the excess temperature profile and calculated the average profile and corresponding standard deviation. Table 1 and the bottom panel of Fig. 1 clearly show that region M1 for the 360 control fields is always cooler than the region M2, exactly the opposite of what is observed for the disk of M 31. Moreover, the temperature of region M1 toward M 31 is always significantly higher than the corresponding temperature of the control fields, and even at four degrees the effect is at  $\approx 4\sigma$ . The same also holds for the region M2: the 360 control fields have a temperature excess of  $66 \pm 10 \mu\text{K}$  at  $4^\circ$ , while the temperature of the region M2 of M 31 is always cooler,  $\approx 32 \mu\text{K}$ . The effect is therefore at  $\approx 3\sigma$  at  $4^\circ$ . We conducted the same study in all the *Planck* bands and found that the results, presented for convenience only for the 100 GHz band here, are similar in each band.

## 2.2. Results for the halo of M 31

Adopting the same geometry as in De Paolis et al. (2011), we estimated the temperature excess in *Planck* sky maps in the region N1+S1 (the region southeast of the halo of M 31 that is expected to be rotating and moving toward the Milky Way if the M 31 halo is rotating along the same axis of the disk) and in the region N2+S2 (the region opposite to the rotation axis). As can be seen from Table 1 and Fig. 2 (upper panel), region N1+S1 is hotter than region N2+S2 at any galactocentric distance. The temperature difference peaks at about  $4^\circ$  (with a value about  $38 \mu\text{K}$ ), but continues up to  $10^\circ$  (where it is still at  $\approx 13 \mu\text{K}$ ).

Beyond about  $12^\circ$ , the temperature asymmetry is inverted and region N2+S2 becomes hotter than region N1+S1 as a result of the intersection with the disk of the Milky Way that clearly is detected in the CMB maps. For the halo of M 31 one can also observe a kind of mirror symmetry between the regions N1+S1 and N2+S2, although it is less pronounced than for the disk of M 31. We also tested whether the measured temperature asymmetry is due to a random fluctuation of the CMB signal by considering 360 control fields with the same shape as regions N1+S1 and N2+S2 at the same latitude of M 31, but at different longitudes (the control fields were equally spaced at one degree distance from each other in longitude). The bottom panel of Fig. 2 shows that for the halo regions (as for the disk of M 31) the temperature asymmetry in the 360 control fields clearly shows an opposite behavior than to the profiles toward M 31 and regions N1+S1 are always cooler than regions N2+S2 (bottom panel in Fig. 2). This effect is clearly due to the presence of the Milky Way in the CMB sky maps, which makes regions N2+S2 generally hotter than the N1+S1 regions. It can be easily observed by comparing the temperature asymmetry profile of the halo of M 31 with that of the control fields that region N1+S1 of M 31 is always hotter than the control field profile (with a confidence level of about  $4\sigma$  at  $4^\circ$  and  $2.7\sigma$  at  $10^\circ$ ), while the region N1+S1 is cooler than the control field profile (with a confidence level of about  $3.7\sigma$  at  $4^\circ$  and  $2.1\sigma$  at  $10^\circ$ ). We therefore conclude that the probability that the asymmetry effect toward the halo of M 31 at 100 GHz is due to a random fluctuation of the CMB signal is well below 1%. We also point out that we have verified that the temperature asymmetry toward the halo of M 31 vanishes if the adopted geometry is rigidly rotated by an angle larger than about  $10^\circ$  with respect to the assumed M 31 rotation axis, which again indicates that the asymmetric halo temperature is a genuine effect due to the halo rotation and not simply a random fluctuation of the CMB signal.

## 2.3. Local Group hot-gas effect

Recently, Rubin & Loeb (2014) raised an interesting question related to the kinetic Sunyaev-Zel'dovich effect from the diffuse hot gas in the Local Group. Because the Local Group moves with respect to the CMB (Rauzy & Gurzadyan 1998), its hot-gas halo component should imprint a non primordial temperature shift in the CMB signal. The expected effect should be detected as a hot spot of a few degree in size in the direction of the M 31 galaxy, which is located opposite to the center of the Local Group. Because of geometrical considerations, the free electron optical depth is highest just toward the M 31 galaxy. On the other hand, in the opposite direction to the M 31 galaxy, the same effect should induce a minimum in temperature in the *Planck* maps of the sky. We investigated this question by searching in the *Planck* sky map at 100 GHz and found (see the last two lines at the bottom of Table 1) that the mean temperature excess in a  $4^\circ$  circle toward the M 31 galaxy is  $\approx 50.1 \pm 0.3 \mu\text{K}$ , which is consistently hotter than the average temperature in the southern hemisphere of the sky ( $\approx 40.5 \mu\text{K}$ )<sup>3</sup>. Toward the anti M 31 direction ( $l = 301.17^\circ$ ,  $b = 21.57^\circ$ ) we found a temperature excess of  $-6.2 \pm 0.3 \mu\text{K}$  in a  $4^\circ$  circle, to be compared with the average temperature in the northern hemisphere of the sky of about  $27.5 \mu\text{K}$ . Like for the disk and halo of M 31, we also considered 360 control fields – this time randomly extracted around (within  $20^\circ$ ) either the M 31 and anti-M 31 directions.

<sup>3</sup> The mean temperature in both the southern and northern hemispheres of the sky was evaluated after the equatorial region, which is affected by the Milky Way emission, was subtracted.

The results obtained are shown in the two lines at the bottom of Table 1 and, obviously, the  $4^\circ$  circle toward M 31 is hotter than the control fields at about  $3\sigma$ . Toward the anti-M 31 direction, the  $4^\circ$  circle is clearly much cooler than the control fields (at about  $29\sigma$ ). The effect predicted toward the M 31 galaxy by Rubin & Loeb (2014) was of a few  $\mu\text{K}$ , and the authors did not mention the possible existence of a cold spot in the anti-M 31 direction. From the discussion above it is clear that the observed temperature difference (about  $56\ \mu\text{K}$ ) between the M 31 and anti-M 31 directions cannot be explained as a random fluctuation of the CMB signal and therefore very probably arises from two main contributions: the kinetic Sunyaev-Zel'dovich effect and the hot gas in the halo of M 31, with a density higher than the average hot-gas density in the Local Group. This hot-gas halo component in M 31, as predicted in De Paolis et al. (1995), might be able to explain both the CMB temperature increase toward the M 31 galaxy and, if it rotates around the same rotation axis as the disk of M 31, the temperature shifts between the two sides of the halo of M 31 as discussed above.

### 3. Conclusions

Galactic halos are more rarely studied than galactic disks, and we still have only incomplete knowledge, not only of the main halo constituents, but also of the degree to which galactic halos rotate with respect to the disks (Courteau et al. 2011; Deason et al. 2011). The rotation of the galactic halos is clearly related to the formation scenario of galaxies. In the standard collapse model (see e.g. Eggen et al. 1962) both the halo and disk originate from the same population, and the rotation of the outer halo should, in this case, be aligned with the disk angular momentum. In contrast, in a hierarchical formation scenario, structures that reach the outer halo later should be less connected to the disk. Therefore, it is evident that information on the galactic halo rotation provides key insights into the formation history of galaxies. It is also well known that the disk of M 31 rotates with a speed of about  $250\ \text{km s}^{-1}$ , which has been clearly shown by the velocity maps obtained from radio measurements as well (Chemin et al. 2009; Corbelli et al. 2010). These maps look very similar to what we found in the *Planck* data toward the disk of M 31. In the previous section we also reported that *Planck* data show a temperature asymmetry with respect to the disk-halo rotation axis, up to a galactocentric distance of about 130 kpc and with a peak temperature contrast of about  $40\ \mu\text{K}$ . Until now, the only evidence

of the rotation of the M 31 halo came from the analysis of the dwarf galaxies that orbit M 31 (Ibata et al. 2013; Veljanoski et al. 2013).

In general, five possibilities may be considered to explain the effects discussed in Sects. 2.1–2.3: (i) free-free emission; (ii) synchrotron emission; (iii) anomalous microwave emission from dust grains; (iv) the kinetic Sunyaev-Zel'dovich effect; and (v) cold gas clouds that populate the halo of M 31. A detailed study of what each of these five possible cause might contribute, using all the *Planck* bands to constrain the model parameters and the relative weight of these five models, will be published elsewhere. Here, we only note that effects (i)–(iii) are strongly wavelength dependent, while (iv) and (v) are almost independent of the observation band in the microwave regime and to first approximation might provide the main contribution to the observed effect. Thus, our investigation shows the power of the CMB to trace, in addition to the clusters of galaxies via Sunyaev-Zeldovich effect and large-scale voids (e.g. Gurzadyan & Kocharyan 2009), also individual galactic halos.

*Acknowledgements.* We acknowledge the use of the Legacy Archive for Microwave Background Data Analysis (LAMBDA) and HEALPix (Górski et al. 2005) package. P.J. acknowledges support from the Swiss National Science Foundation.

### References

- Bersanelli, M., Mandolesi, N., Butler, R. C., et al. 2010, *A&A*, 520, A4  
 Binney, J., & Merrifield, M. 1998, *Galactic Astronomy*, Princeton Series in Astrophysics (Princeton: Princeton University Press)  
 Burigana, C., Davies, R. D., De Bernardis, P., et al. 2013, *Int. J. Mod. Phys. D*, 22, 1330011  
 Chemin, L., Carignan, C., & Foster, T. 2009, *ApJ*, 705, 1395  
 Corbelli, E., Lorenzoni, S., Walterbor, R., et al. 2010, *A&A*, 511, A89  
 Courteau, S., Widrow, L. M., McDonald, M., et al. 2011, *ApJ*, 739, 20  
 De Paolis, F., Ingrosso, G., Jetzer, Ph., et al. 1995, *A&A*, 299, 647  
 De Paolis, F., Gurzadyan, V. G., Ingrosso, G., et al. 2011, *A&A*, 534, L8  
 Deason, A. J., Belokurov, V., & Evans, N. W. 2011, *MNRAS*, 411, 1480  
 Eggen, O. J., Lynden-Bell, D., & Sandage, A. R. 1962, *ApJ*, 136, 748  
 Górski, K. M., Hivon, E., Banday, A. J., et al. 2005, *ApJ*, 622, 759  
 Gurzadyan, V. G., & Kocharyan, A. A. 2009, *A&A*, 493, L61  
 Ibata, R. A., Lewis, G. F., Conn, A. R., et al. 2013, *Nature*, 493, 62  
 Lamarre, J. M., Puget, J. L., Ade, P. A. R., et al. 2010, *A&A*, 520, A9  
 Planck Collaboration 2012, *A&A*, 543, A102  
 Rauzy, S., & Gurzadyan, V. G. 1998, *MNRAS*, 298, 114  
 Rubin, D., & Loeb, A. 2014, *JCAP*, 01, 051  
 Veljanoski, J., Ferguson, A. M. N., Mackey, A. D., et al. 2013, *ApJ*, 768, L33  
 Vilardell, F., Ribas, I., Jordi, C., Fitzpatrick, E. L., & Guinan, E. F. 2010, *A&A*, 509, A70